FEATURES OF CONTACT AND SURFACE PROCESSES IN GLASSY $As_2Te_{13}Ge_8S_3$-BASED STRUCTURES WITH Pt ELECTRODES UPON INTERACTION WITH NITROGEN DIOXIDE

Marina Ciobanu

Department of Physics, Technical University of Moldova, bld. Dacia 41, Chisinau, MD-2060 Republic of Moldova
E-mail: ciobmarina@gmail.com

(Received August 3, 2017)

Abstract

The capacitance spectra of the interdigital Pt–glassy $As_2Te_{13}Ge_8S_3$–Pt structures have been investigated in a range of 5–10^6 Hz with respect to temperature effects in both dry air and its mixture with a controlled concentration of nitrogen dioxide. It has been found that a decrease in the frequency of applied voltage to 10^3 Hz results in a rapid increase in the capacitance by several orders of magnitude. Environmental conditions dramatically influence the capacitance at low frequencies and, together with temperature regime, control the capacitance spectra and current–voltage characteristics of the films. The results are explained in terms of formation of a Schottky–Mott barrier that controls the properties of the contact junction. The contact-free part of the chalcogenide film surface, being more conducting than the bulk, acts as a capacitor, which can be controlled by interaction with gaseous species from the environment.

1. Introduction

Tellurium-based thin films are of great interest due to their high electrical sensitivity to surface processes induced by interaction with environmental gaseous species [1, 2]. This interaction affects both the electric resistivity [3, 4] and impedance [5, 6] of the films, being controlled by alloys composition [7], fabrication technology [8], the nature and concentration of gaseous species [9], annealing [10],temperature regime of operation [11], and so on. Recently, we have shown the high sensitivity of both impedance and work function of quaternary Te-based thin films to nitrogen dioxide, as well as the cross sensitivity to water vapour and other gases, at room temperature [12, 13]. It is strange, but so far, there have been no communications concerning the effect of gas adsorption on capacitance of these films, although the experimental specimens usually consist of a layer of a chalcogenide-based film enclosed between metallic electrodes in a "sandwich," "planar," or interdigital design. Apparently, this fact is attributed to a high value of dielectric relaxation time of disordered chalcogenides materials, including the Te-based ones, which leads to the independence of metal–chalcogenide glassy semiconductor (ChGS) junctions of frequency, the phenomenon observed already at early stages of investigation of these materials [14]. On the other hand, in some cases, a strong increase of capacitance of the metal–ChGS–metal structures at low frequencies occurs. This effect was observed in structures based on both As_2S_3 and Sb_2S_3 with nonsymmetric electrodes made of Al and Au [15] as well as in either aged or annealed Au–$Ge_{16}As_{35}Te_{28}S_{21}$–Au structures [16]. In both cases, this behaviour was analysed by assuming that, with a decrease in frequency, the period of applied voltage variation becomes comparable to a dielectric relaxation time. It was concluded that, in both cases,

at high frequencies, the capacitance corresponds to a geometric capacitor with a ChGS as a passive insulator; however, at low frequencies, the capacitance is controlled by a high-resistance layer adjacent to the contacts. The high resistive layer at the Al–As_2S_3(Sb_2S_3) contact was found to be a Schottky barrier; however, at the Au–$Ge_{16}As_{35}Te_{28}S_{21}$ contact, it is an alloying layer produced by aging or annealing. Later, it was demonstrated that the capacitance of Al–ChGs (As_2Se_3) is very sensitive to the prehistory and ambient environment in which the experiment is conducted [17].

The present work is focused on the investigation of the effect of frequency of applied voltage and toxic (e.g., NO_2) gases on the capacitance of thin film layers of quaternary glassy chalcogenides with Pt interdigital electrodes. For an unambiguous interpretation of the results, the effect of temperature on the capacitance spectra is also considered.

2. Experimental

Glassy alloy $As_2Te_{13}Ge_8S_3$, obtained by the procedure described in [12, 13], was used as the primary material for growing the relevant thin-film structures. The films were grown by thermal “flash” evaporation of the original material in a vacuum from tantalum boats onto sintered alumina ceramic substrates containing previously deposited platinum interdigital electrodes produced by SIEMENS AG with an electrode width of 15 μm and interelectrode distances of 45 μm. The growth velocity of the film was on the order of 30 nm/s; the area of deposition was about 5 mm^2. Structural investigations were carried out by X-ray diffraction analysis using a DRON YM1 diffractometer using FeK_α radiation; the surface morphology of the films was made visible with a VEGA TESCAN TS 5130 MM scanning electron microscope (operating voltage 30 kV). The films were encapsulated in standard TO-8 sockets, and their contacts were thermally bonded to socket pins by means of copper wires. The sockets with thin-film devices were placed into a test cell (volume of 10 mL), which was combined with an electrical refrigerator allowing cooling the sample to 10°C. These two pieces were together contained in an electric furnace for heating and regulating the operating temperature of the film. A platinum resistance temperature detector PT-100 close to the film was used for assisting the temperature control.

A gaseous NO_2 mixture with a concentration of 1.5 ppm was obtained with a calibrated permeation tube (Vici Metronics, United States), which was incorporated into the experimental setup described elsewhere. Dry air was used as the carrier and reference gas. The capacitance of the films was measured either in air or in a gaseous nitrogen dioxide environment in a frequency range of 5 Hz to 13 MHz, using an HP 4192A impedance analyzer. The same samples were used for both the frequency and temperature effect studies.

The gases were injected parallel to the film surface using a flow rate of 100 mL/min. The experiments were accomplished as follows:

(a) Measurement of C–ω characteristics at a lower (11°C) temperature in pure air and in gaseous media with different concentration of NO_2.

(b) Heating to room temperature and performing the measurements of capacitance spectra in pure air and in gaseous media with NO_2 again.

(c) This cycle of measurements was repeated at temperatures 38 and 53°C.

Additionally, the current–voltage (*I*–*U*) characteristics were measured in normal ambient at different temperatures. The measurements were performed in a quasi-stationary regime: the applied voltage varied between –6.0 V and +6.0 V in steps, increasing by 20 mV at each step, while the respective values of the current were measured. The delay time between two

measurements was 2 s. The measurements were performed at temperatures between 25 and 100°C.

3. Results and Discussion

3.1. Film morphology and structure

Figure 1a shows the surface morphology of a $As_2Te_{13}Ge_8S_3$ film with interdigital Pt electrodes physically grown by evaporation in a vacuum onto sintered Al_2O_3 substrates. It is evident that the film shows a great surface roughness; however, no crystalline tracks are observed. The last fact is confirmed by Fig. 1b, where a portion of the ChGS film from interdigital space is shown at a 10^3 higher magnification. The sample surface consists of typical interconnected agglomerates of islands at micrometric scale [12]. No crystalline tracks were observed from XRD spectra analysis either; these findings are consistent with the results published in my previous work [18].

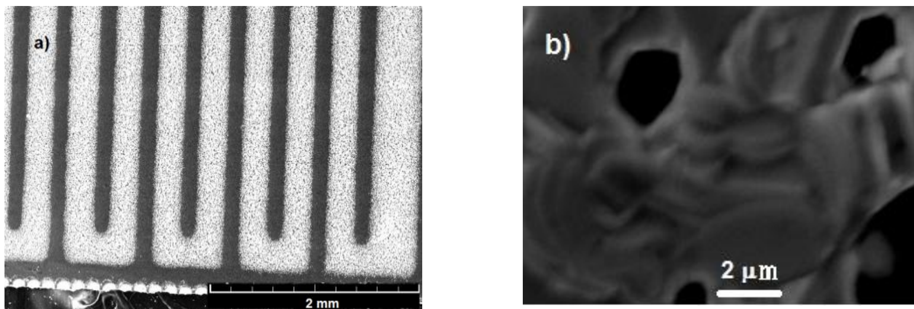

Fig. 1. (a) SEM of an $As_2Te_{13}Ge_8S_3$ film with interdigital Pt electrodes and (b) the morphology of the ChGS surface magnified by 10^3 times.

3.2. Capacitance in normal ambient

The dependence of capacitance of the Pt–$As_2Te_{13}Ge_8S_3$–Pt structure on the frequency of applied voltage at $22^{\circ 0}$C in normal ambient is shown in Fig. 2. It is seen that the capacitance, being independent of frequency at $\omega > 10^4$ Hz, sharply increases by several orders of magnitude at lower frequencies. Obviously, the constant value of capacitance at frequencies higher than 10^4 corresponds to geometric capacitor $C_h = \varepsilon\varepsilon_0 S / d$, where d and ε are the interdigital distance and permittivity of ChGS, respectively, and S is the contacting aria. The rapid and huge increase in the capacitance with a frequency decrease lower than 10^4 Hz indicates the existence of narrow high resistive regions near contacts and the equalization of dielectric relaxation time $\tau_r = \varepsilon\varepsilon_0\rho$ (ρ is the resistivity of the film) with the period of applied voltage variation. As mentioned above, the high resistive regions at the contacts can be attributed either to the depletion of majority carriers near the surface or to the formation of narrow insulating layers at the interface. This statement was partially confirmed by measurements of current–voltage characteristics. The insert in Fig. 2 shows the *I–U* characteristics measured at several temperatures. It is evident that the curves really show a weak rectification that appears to be

symmetric relative to the polarity of the applied voltage regardless of temperature. This result gives evidence that the symmetric contact barriers are formed by the two sides of the ChGS film. These barriers control the total structure capacitance at a low frequency of the applied voltage, that is $C_l = \varepsilon\varepsilon_0 S / (L_1 + L_2)$, where the L_1 and L_2 are the width of high resistive regions.

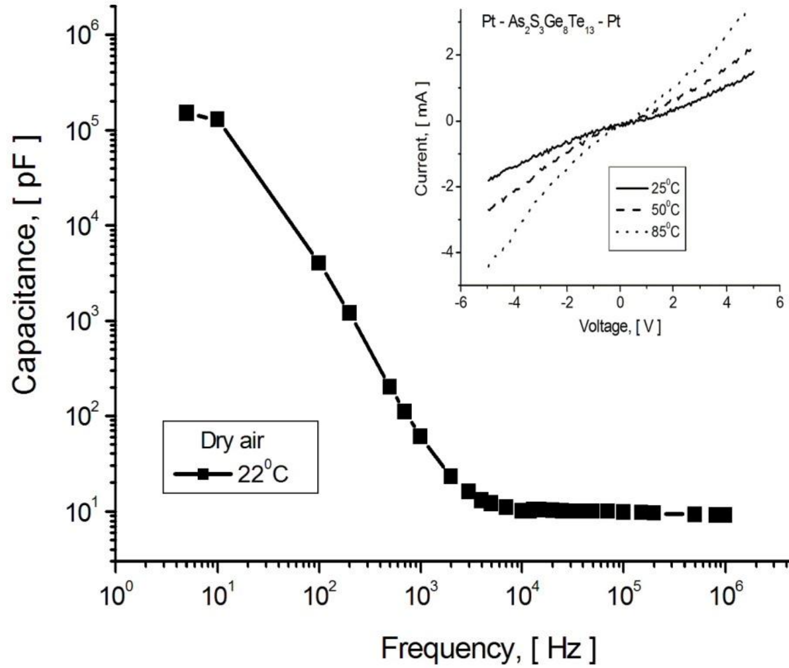

Fig. 2. Capacitance spectra of Pt–$As_2Te_{13}Ge_8S_3$–Pt structures in normal ambient. The insert shows the current–voltage characteristics at different temperatures.

The huge increase in the capacitance—by more than 4 orders of magnitude—at low frequencies (<10^4 Hz) indicates the low width of high resistive regions by the contacts, which, in principle, is also confirmed by the weak rectification.

On the other hand, the transition from geometric capacitance (C_h) to contact (C_l) ones can be implemented only under conditions of equalization (or overcoming) of the period of applied voltage variation with dielectric relaxation time τ_r. As the τ_r value decreases with increasing temperature (see insert in Fig. 2), it is reasonable to expect the frequency-dependent enhancement of capacitance owing to sample heating, especially at low frequencies. Figure 3 shows the capacitance–frequency dependence of structures in question at several temperatures. The inset in this figure illustrates the effect of temperature on the structure capacitance for several frequencies of applied voltage. It is evident that, at low frequencies, the structure capacitance increases with increasing temperature.

Thus, the structure capacitance increases either owing to raising the temperature at a fixed frequency or owing to lowering the frequency at a fixed temperature. In both cases, the effect is due to a reduction in the dielectric relaxation time caused by an increase in the ChGS

conductivity.

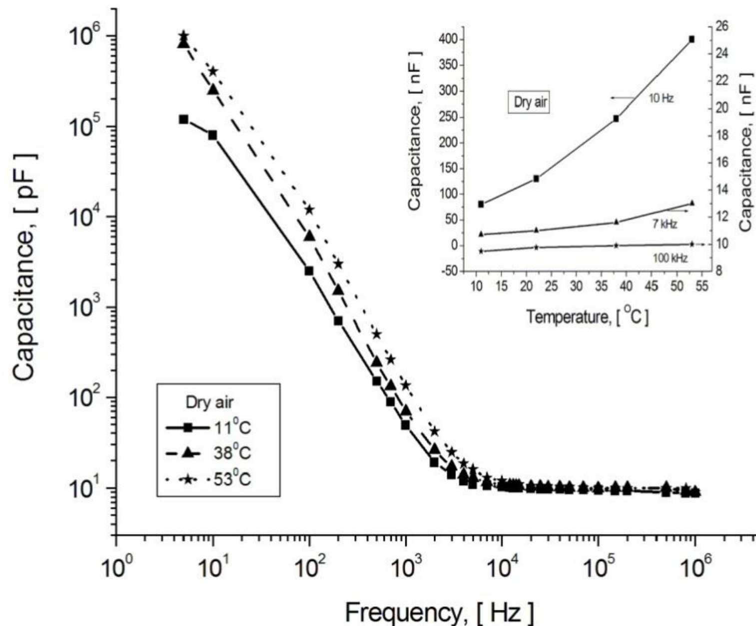

Fig. 3. Capacitance versus frequency of applied voltage at different temperatures. The insert shows the temperature dependence of capacitance in dry air.

In principle, it means the temperature-induced shift of the rising edge of capacitance spectra toward higher frequencies. We observed that this shift—much enhanced—can be also induced by a change in the ambient environment.

3.3. Effect of gas adsorption

Capacitance measurements for a Pt–$As_2Te_{13}Ge_8S_3$–Pt structure showed that a change in the ambient environment from dry air to a mixture containing even a very small concentration of nitrogen dioxide has a significant effect on the *C*–ω characteristics. Figure 4 shows the frequency dependence of a sample in question at room temperature in both dry air and its mixture with 1.5 ppm of NO_2. It is seen that, although the target gas does not modify the shape of the *C*–ω spectra, it leads to an increase in the sample capacitance in a definite frequency range by approximately 100 times. This effect looks like a strong gas-induced shift of the rising edge of capacitance spectra toward higher frequencies. In addition, note that the adsorption of the gas (e.g., NO_2) affects the capacitance of the structure precisely at low frequencies, that is, in a frequency range where the sample capacitance is assumed to be controlled by high resistive barriers at the contacts. This behavior is analyzed by assuming the equivalent circuit inserted in Fig. 4.

The equivalent circuit of the Pt–$As_2Te_{13}Ge_8S_3$–Pt structure can be represented by a parallel combination of the bulk resistance (R_b) and capacitance (C_b) connected in parallel with a further parallel combination of the surface resistance (R_s) and capacitance (C_s). As the device

structure has a planar design (Fig. 1a), there is also a parallel combination of the resistance (R_c) and capacitance (C_c) corresponding to thin insulating layers usually formed at the contacts put in series with the above mention circuit.

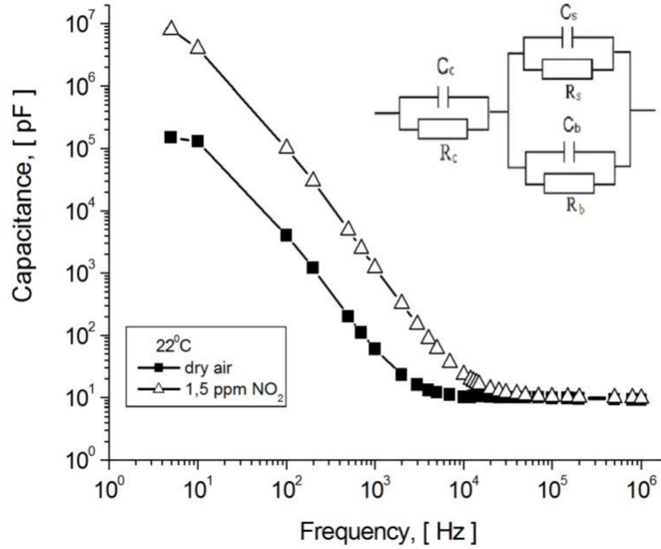

Fig. 4. Variation in the capacitance of the Pt–$As_2Te_{13}Ge_8S_3$–Pt structure with frequency by different ambient environments at room temperatures. The insert shows the equivalent circuit used for analysis.

Let us consider all the components of this equivalent circuit separately. According to many experimental works, including our previous one [13], it is generally accepted that amorphous semiconductors exhibit a tendency of forming a space-charge layer near the surface, which is more conducting as the bulk; that is, by the surface the bands bend up, as shown in Fig. 5a. This effect is due to the interaction of lone-pair electrons of chalcogenide atoms with dangling bonds on the surface. The screening length can be calculated by the standard expression:

$$\lambda = \left(\varepsilon\varepsilon_o / q^2 N_F\right)^{1/2}, \quad (1)$$

where N_F is the density of localized states at the Fermi level and q is the electronic charge. Assuming that $N_F \cong 1,3 \cdot 10^{21} eV^{-1} cm^{-3}$ [19], we found that the value of the screening length (λ) is as low as a few dozens of Angstroms. Under these conditions, the dielectric relaxation time of the layer adjacent to the surface is shorter than that of the bulk; consequently, surface capacitance C_s cannot control the device capacitance at high frequencies.

The same can be argued for capacitance C_c corresponding to thin insulating layers at the contacts (Fig. 5b). The formation of a thin (10–100 Å) insulating layer at the metal–ChGS interface, as well as the major role of surface states at this interface, has been proved by very weak dependence of contact barrier height on work function of the metal [17, 20].

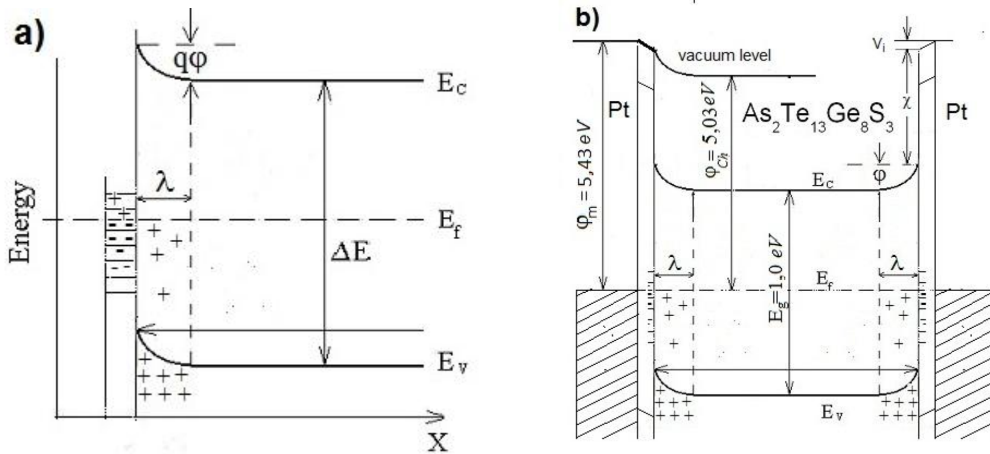

Fig. 5. (a) Energy band model of the ChGS surface and (b) the possible band diagram of the Pt–$As_2Te_{13}Ge_8S_3$–Pt structure with thin insulator layers and surface states at the interfaces.

The theoretical model for this Schottky–Mott barrier is known as the Bardeen model, which, in addition to many remarkable features, assumes that the contact insulating layer can be transparent for carriers due to the tunnelling effect [21]. According to the small thickness of the contact insulating layer, it can be assumed that $C_c >> C_b$ and, at high frequencies, the total capacitance can be approximated as $C_h = C_c C_b / C_c + C_b \approx C_b$. The asymptotic values for low-frequency capacitance derived using the approach of Wey [16] are as follows:

$$C_l = C_c R_c^2 / (R_c + \frac{R_s R_b}{R_s + R_b})^2 \tag{2}$$

Assuming that $R_c \ll R_s \ll R_b$:

$$C_l \approx \frac{C_c R_c^2}{R_s^2} \tag{3}$$

This expression shows that the low-frequency capacitance should quite strongly increase with increasing surface conductance; this finding meets the above presented experimental results. The fact of increase in the conductivity of $As_2Te_{13}Ge_8S_3$ owing to the adsorption of the gas (e.g., NO_2) was clearly demonstrated in our recent works [22, 23]; therefore, the noticeable increase in capacitance induced by interaction with NO_2 molecules (Fig. 4) is due namely to this reason.

4. Conclusions

The capacitance spectra and current–voltage characteristics of the Pt–$As_2Te_{13}Ge_8S_3$–Pt structure indicate the formation of Schottky–Mott contact barriers with narrow insulating layers

at the interfaces. The huge increase in the capacitance with a decrease in frequency below 10^4 Hz is attributed to these narrow high resistive regions near contacts and the equalization of the dielectric relaxation time of $As_2Te_{13}Ge_8S_3$ with the period of applied voltage variation. The capacitance spectra in the low-frequency range are significantly affected by ambient environment. In particular, the application even of a very low concentration (a few units of ppm) of nitrogen dioxide results in a frequency-dependent increase in the capacitance by a few hundreds of times. This finding gives evidence that the surface phenomena control the electric properties of ChGS in question and, in this particular case, the contact-free part of the film surface, which is more conducting than the bulk, acts as a capacitor, which is controlled by interaction with gaseous species from the environment.

Acknowledgments. This work was financially supported by Technical University of Moldova through Institutional Grant 15.817.02.29A. The author wishes to thank Prof. D. Tsiulyanu for stimulating interest and helpful discussions, expressing her gratitude to Dr. M. Enache from NCMST of TUM for SEM analysis and Dr. G. F. Volodina from IAP ASM for XRD analysis.

References

[1] S. I. Marian, D. I. Tsiulyanu, and H.-D. Liess, Sens. Actuators, B 78, 191 (2001).
[2] J. P. Reithmaier et al., Nanotechnological Basis for Advanced Sensors, Springer, Dordrecht, The Netherlands, 2011.
[3] D.Tsiulyanu et al.,Thin Solid Films 485, 252 (2005).
[4] T. Siciliano et al. , Sens. Actuators, B 135,250 (2008).
[5] S. Sen et al., Sens. Actuators, B 115, 270 (2006).
[6] D. Tsiuleanu and O. Mocreac, J. Non-Oxide Glasses, 3, 37 (2011).
[7] J.Wüsten and K.Potje - Kamloth, Sens. Actuators, B 145, 216 (2010).
[8] V. Bhandarkar et al., Mater. Sci. Eng. B131,156 (2006).
[9] D. Tsiulyanu et al., Sens. Actuators, B 121,406 (2007).
[10] S.-K. Duk and D.-D. Lee, Mater. Res. Soc. Symp. Proc. 828, A7.1.1 (2005).
[11] D. Tsiulyanu et al., Sens. Actouators , B 100, 380 (2004).
[12] D. Tsiulyanu and M. Ciobanu , Sens. Actuators, B 223, 95(2016) .
[13] D. Tsiulyanu, M. Ciobanu, and H.- D. Liess, Phys. Status Solidi, B, 253, 1046 (2016).
[14] V.M. Lyubin and V.S. Maidzinski, Fiz.Tverd. Tela, 6,3740(1964).
[15] A.A. Simashkievici and S.D. Shutov, Phys. Status Solidi (a), 343, (1984).
[16] H. Y. Wey, Phys. Rev. B, 13, 3495 (1976).
[17] M. Popescu, A. Andriesh, V. Chiumach, M. Iovu, S. Shutov, and D. Tsiulyanu, The Physics of Chalcogenide Glasses, Ed. Stiintifica Bucharest-IEP Stiinta, Chisinau, 1996, 488 p.
[18] M. Ciobanu**,** Proc. 5th Conference of doctorates, ASM, Chisinau, 2016, p. 22–27.
[19] M. Ciobanu and D.Tsiulyanu, Abstr. 8th Int. Conf. MSCMP, Chisinau, 2016, p. 99.
[20] D.I. Tsiulyanu, Soviet Physics—Semiconductors (English Translation) 22,749 (1988).
[21] E. Rhoderick, Kontakty metall–provodnik, Radio Svyaz, Moscow, 1982, 209 p.
[22] D. Tsiulyanu and M. Ciobanu, Proc. 3rd Int. Conf. Nanotechnologies and Biomedical Engineering, Springer, Berlin, 55, 382, (2016).
[23] M. Ciobanu, Abstr. 8th Int. Conf. Amorphous and Nanostructured Chalcogenides, Sinaia, Romania, 2017, p. 8.